

Role of Met80 and Tyr67 in the Low-pH Conformational Equilibria of Cytochrome *c*

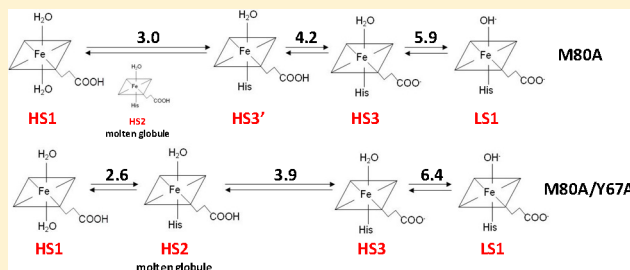
Gianantonio Battistuzzi,^{*,†} Carlo Augusto Bortolotti,[†] Marzia Bellei,[†] Giulia Di Rocco,[†] Johannes Salewski,[‡] Peter Hildebrandt,[‡] and Marco Sola[†]

[†]Department of Chemistry, University of Modena and Reggio Emilia, via Campi 183, 41100 Modena, Italy

[‡]Technische Universität Berlin, Institut für Chemie, Sekr. PC14, Straße des 17. Juni 135, D-10623 Berlin, Germany

Supporting Information

ABSTRACT: The low-pH conformational equilibria of ferric yeast iso-1 cytochrome *c* (ycc) and its M80A, M80A/Y67H, and M80A/Y67A variants were studied from pH 7 to 2 at low ionic strength through electronic absorption, magnetic circular dichroism, and resonance Raman spectroscopies. For wild-type ycc, the protein structure, axial heme ligands, and spin state of the iron atom convert from the native folded His/Met low-spin (LS) form to a molten globule His/H₂O high-spin (HS) form and a totally unfolded bis-aquo HS state, in a single cooperative transition with an apparent pK_a of ~ 3.0 . An analogous cooperative transition occurs for the M80A and M80A/Y67H variants. This is preceded by protonation of heme propionate-7, with a pK_a of ~ 4.2 , and by an equilibrium between a His/OH[−]-ligated LS and a His/H₂O-ligated HS conformer, with a pK_a of ~ 5.9 . In the M80A/Y67A variant, the cooperative low-pH transition is split into two distinct processes because of an increased stability of the molten globule state that is formed at higher pH values than the other species. These data show that removal of the axial methionine ligand does not significantly alter the mechanism of acidic unfolding and the ranges of stability of low-pH conformers. Instead, removal of a hydrogen bonding partner at position 67 increases the stability of the molten globule and renders cytochrome *c* more susceptible to acid unfolding. This underlines the key role played by Tyr67 in stabilizing the three-dimensional structure of cytochrome *c* by means of the hydrogen bonding network connecting the Ω loops formed by residues 71–85 and 40–57.



Conformational changes in proteins caused by binding events and/or modification of the properties of the medium are essential for biological functions.^{1–5} Moreover, biotechnological applications of proteins may rely on reversible conformational transitions associated with changes in property and function (biomolecular switches).^{6–9} Therefore, elucidating the trigger event(s) and the mechanism of conformational equilibria in proteins has a fundamental and applicative relevance.⁴ The conformational equilibria leading to non-native states of cytochrome *c* (cytc) have been studied in depth,^{10,11} as they are likely involved in some as yet not fully understood functions of cytc beyond electron transfer, such as apoptosis and cellular oxidative stress.^{13–20} Moreover, cytc has been widely used as a model to gain information about the mechanism of protein folding and unfolding processes.^{21–34} The effects of pH on cytc structure and function have been extensively investigated.^{10,35} The low-pH conformational changes start with disruption of the axial methionine–Fe(III) bond and formation of a molten globule state, followed by extensive protein unfolding.^{10,29,35–52} This complex process is affected by the ionic strength and the nature of the anions in solution,^{4,29,36–44,46,47,49–52} which influence heme coordination and the structure and stability of the protein conformers. Indeed, the molten globule state is stabilized at high ionic

strengths, while at low salt concentrations, the acid transition appears as a single cooperative transition between the native and low-pH unfolded forms.^{4,29,36–39,42–44,46,49,50} In the latter case, the nature of the axial heme iron ligands is still debated.^{4,51} It is known that cytc at low pH displays a peroxidase-like activity,⁵³ which at neutral pH can be obtained by replacing the axial Met80 with a noncoordinating Ala.^{54–56} Moreover, upon binding to cardiolipin *in vivo*, cytc acts as a cardiolipin oxygenase and peroxidase, thus playing a role in the apoptotic events in mitochondria.^{12,18–20} The conserved Tyr67 was proposed as a possible apoptotic trigger.⁵ Indeed, Tyr67 plays a key role in stabilizing the three-dimensional (3D) structure of cytc at pH 7, as its OH group participates in the hydrogen bond (H-bond) network in the distal side of the heme connecting the Ω loop containing Met80 (from residue 71 to 85) with that formed by residues 40–57,^{5,57–63} which is the least stable part of cytc and triggers both acid and alkaline unfolding.^{27,31,48,64,65} *Saccharomyces cerevisiae* cytochrome *c* is not involved in apoptosis. However, investigating the low-pH conformational transition in yeast cytc mutated at Met80 and

Received: June 4, 2012

Revised: July 6, 2012

Published: July 9, 2012



Tyr67 can contribute to the understanding of the role that these residues play in stabilizing cytc conformation.

Electronic absorption spectra provide information about the spin state, oxidation state, and coordination number of the iron atom in heme proteins.^{66–68} However, elucidation of the molecular processes associated with pH-induced conformational equilibria requires methods that are more sensitive to structural changes of the heme center and its protein environment, such as magnetic circular dichroism (MCD)^{68–89} and resonance Raman (RR) spectroscopies.^{4,46,80,81,90,91}

In this work, the spectral properties of oxidized wild-type (wt) yeast iso-1 cytochrome *c* (ycc) and its M80A, M80A/Y67A, and M80A/Y67H mutants (Figure 1) were investigated

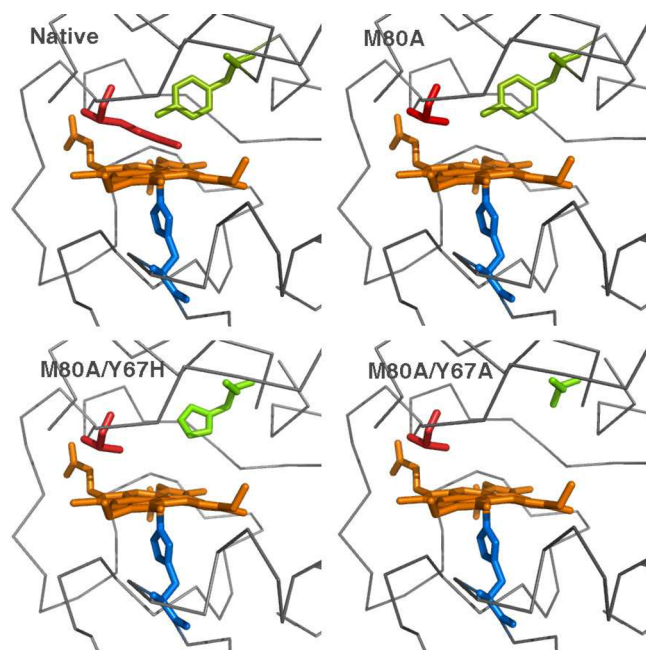


Figure 1. Heme cavity in wild-type, M80A, M80A/Y67H, and M80A/Y67A *S. cerevisiae* cytochrome *c*. Structural data are from Protein Data Bank entries 1YCC (native cytc) and 1FHB (M80A variant).

from pH 7 to 2 at low ionic strength. The analysis of the spectral data offers new insight into the pH-dependent axial heme ligand swapping and conformational equilibria of mitochondrial cytochrome *c* and into the crucial role of Tyr67 in stabilizing the folding of cytc. Furthermore, it contributes to a comprehensive understanding of the electronic and structural properties of the heme group in non-native states of the protein imparted with biologically relevant peroxidase-like activity.

EXPERIMENTAL PROCEDURES

Materials. All chemicals were of reagent grade. Doubly distilled water was used throughout this work.

Protein Production and Isolation. Wild-type recombinant *S. cerevisiae* iso-1 cytochrome *c* and its M80A, M80A/Y67H, and M80A/Y67A mutants were expressed and isolated as described previously.^{53–56} All protein variants are non-trimethylated and carry the C102T mutation, to prevent protein dimerization.⁵⁶

Spectroscopic Measurements. Electronic absorption and MCD spectra were recorded in the Soret (360–450 nm) and

visible (450–710 nm) regions with a Jasco J-810 spectropolarimeter. The magnetic field was provided by a GMW Magnet system model 3470 split coil superconductivity magnet with a maximum field of 1 T (T). The MCD spectra were measured in $[\theta]$ (millidegrees) and converted to $\Delta\epsilon$ ($\text{M}^{-1} \text{cm}^{-1} \text{T}^{-1}$) using the conversion factor $\Delta\epsilon = \theta / (32980c d B)$, where c is the protein concentration, B is the magnetic field (1 T), and d is the thickness of the sample (path length, 0.2 cm).⁶⁹ All experiments were conducted at 25 °C with protein solutions freshly prepared before use in 0.5 mM phosphate buffer (pH 7), and the protein concentration was checked spectrophotometrically, using an ϵ_{410} of $106100 \text{ M}^{-1} \text{cm}^{-1}$ for the wild-type protein and an ϵ_{405} of $121700 \text{ M}^{-1} \text{cm}^{-1}$ for the M80A, M80A/Y67A, and M80A/Y67H mutants.^{92,93} RR spectra were obtained with 413 nm excitation (Krypton ion laser, Coherent Innova 300c) using a confocal Raman spectrometer (Jobin Yvon, LabRam 800 HR) equipped with a liquid nitrogen-cooled back-illuminated CCD detector. The total acquisition time for each spectrum was between 300 and 1600 s with a wavenumber increment per pixel of $\sim 0.4 \text{ cm}^{-1}$. The laser beam (3–10 mW) was focused onto the sample contained in a rotating cuvette using a Nikon 20 \times objective (N.A. 0.35) with a working distance of 20 mm.⁹¹ For RR experiments, protein concentrations were $\sim 150 \mu\text{M}$. The pH of the samples was changed by adding small amounts of concentrated HCl under fast stirring.

RESULTS AND DISCUSSION

Wild-Type Cytochrome *c*. The UV–vis and MCD spectra of ferric wt ycc are essentially pH-insensitive between pH 7.0 and 4.0 and coincide with those for horse heart cytc at pH 7.0 (Figure S1 of the Supporting Information and Table 1).^{76,80,86,93,94} The MCD derivative-shaped signals in the Soret and in the visible regions are typical of a low-spin (LS) six-coordinate (6c) ferric heme,^{76,77,80,93} as expected from the His/Met axial heme iron ligation.^{10,11} When the pH is reduced to <3.5 (Figure S1 of the Supporting Information and Table 1), the Soret band increases in intensity and shifts to shorter wavelengths (an isosbestic point is observed at 404 nm), while the peak and the trough of the corresponding MCD signal are weakened and shift to shorter wavelengths. At the same time, in the visible part of the spectra, the intensities of the absorption bands at 528 and 555 nm decrease, the peak-to-trough distance of the S-shaped MCD signal decreases, and a charge-transfer band and a new MCD trough are observed at 618 and 632 nm, respectively (Figure S1 of the Supporting Information and Table 1). The features at pH 2.7 indicate that the heme of ycc progressively shifts to a predominantly 6c high-spin (HS) state, in agreement with NMR data.⁹⁵ With the decrease in pH to 2.0, the Soret band and the corresponding MCD signal undergo a further blue shift with an isosbestic point at 400 nm, concomitant with a red shift of the charge-transfer band to 617 nm, and a new absorption band at 492 nm replaces those at 528 and 555 nm (Figure S1 of the Supporting Information and Table 1). These spectral changes closely parallel those of horse heart cytc^{4,36–39,41–44,46,47,50,96} and are consistent with the presence of three different conformers below pH 4,^{4,36–39,41–44,46,47,50,96} involved in two conformational equilibria.^{4,36–39,41–44,46,47,50,51} The LS His/Met-ligated form (LS1) converts upon Met swapping by a water molecule to a HS-heme containing molten globule conformer (HS2),^{4,36–38,50,51,97} prevailing from pH 3.4 to 2.6, which represents a globular and compact state with a high content of

Table 1. Wavelengths of the Relevant Spectral Features of the UV–Vis and MCD Spectra of *S. cerevisiae* Cytochrome *c* and Its M80A, M80A/Y67H, and M80/Y67A Variants as a Function of pH^a

variant	species	pH	MCD						absorption	
			Soret			vis			Soret	vis
			peak	trough	zerocross	peak	trough	zerocross		
wt	LS1	7.0	401	415	409	548	567	556	408	528, 555
	HS2	2.7	393	414	404	545	545, 567, 632		396	528, 555, 618 _{CT}
	HS1	2.0	389	402	396		550, 629		394	492, 530 _s , 617 _{CT}
M80A	LS1	7.3	399	413	407	554	574, 539	561	405	532, 554
	HS3	5.0	398	413	406	553	536, 570, 630	559	402	526, 557, 621 _{CT}
	HS3'	4.0	397	412	406	553	535, 567, 629	558	401	524, 557, 621 _{CT}
	HS2	3.3	395	411	404	553	535, 565, 629	558	398	522, 556, 620 _{CT}
	HS1	2.0	390	402	397	554	539, 565, 628	547, 558	394	491, 525 _s , 556, 617 _{CT}
M80A/Y67H	LS1	7.0	399	413	407	548	574	559	405	532, 563
	HS3	5.0	398	414	406	549	565, 572, 628	555	402	524, 563, 617 _{CT}
	HS3'	3.9	397	412	406	548	565, 572, 628	554	401	524, 563, 617 _{CT}
	HS2	3.0	395	411	405	548	566, 570, 630	555	398	524, 563, 614 _{CT}
	HS1	2.0	390	402	398	—	537, 564, 630		394	491, 524 _s , 563, 616
M80A/Y67A	LS1	7.0	398	413	406	560, 552	573	566	405	533, 562
	HS3	4.9	398	413	405	550	572, 630	562	402	527, 562, 622 _{CT}
	HS2	3.4	395	411	404	550	572, 629	560	398	527, 562, 622 _{CT}
	HS1	1.9	391	402	397		538, 564, 627		394	491, 525 _s , 560, 617 _{CT}

^aSpectra were recorded in 0.5 mM phosphate buffer at different pH values. Protein concentrations ranged from 17 μ M to 0.15 mM. Subscripts s and CT stand for shoulder and charge transfer, respectively.

ordered secondary structure and a fluctuating tertiary conformation.^{32,33,49–51} These spectra at low ionic strengths are closely similar to those for *N*-acetyl microperoxidase-8 and -11 at pH 7, which include a His/H₂O axially ligated HS heme.^{66,67,98} The presence of this coordination state in the HS2 conformer is in line with literature data for horse heart cytc that show that the HS form of the molten globule species prevails at low ionic concentrations.^{37,38,50,97} Below pH 2.6, a new conformer, HS1 prevails that still contains a predominantly 6c HS heme, as the Soret band is sensibly narrower and more intense than that for 5c heme^{67,68} and the corresponding MCD signal has a typical S shape (Figure S1 of the Supporting Information).^{68,76–78,80–86,88,89,99} This conformer would correspond to the totally unfolded form. The absorption spectrum at pH 2 almost coincides with those of *N*-acetyl microperoxidase-8 and -11 under the same conditions, which contain a 6c HS heme with a H₂O/H₂O axial ligation,^{66,67,98,100} while some differences exist compared to the state of horse cytc at pH 2 in the presence of 9 M urea, which includes a H₂O and His as axial ligands.⁸⁰ Therefore, at this pH, two water molecules most likely bind axially to the heme iron in HS1, although minor contributions of a His/H₂O-ligated HS heme cannot be excluded, as indicated by resonance Raman studies.^{4,47} Horse heart cytc at pH 1.8 displays different MCD spectra,⁷⁶ likely because of the effects of a high concentration of Cl[–] (0.6 M) that induce a mixed spin-state population.⁷⁶

The pH-dependent changes in the peak-to-trough distance of the MCD Soret signal (Figure 2a) and in the absorbance of the Soret band for the LS1 (408 nm) and HS1 (394 nm) conformers of wt ycc (Figure 2b,c) indicate that the electronic properties of the heme are influenced by a single acid–base equilibrium (Scheme 1). The absorbance and peak-to-trough changes versus pH profiles can be described well on the basis of a one-proton equilibrium yielding an average pK_a value of 3.0 \pm

0.2 for the overall HS1 to LS1 transition, which compares favorably to previously reported values for native and wt recombinant yeast cytochrome *c*.^{65,101} The value is slightly higher than the respective pK_a of horse heart cytc (2.5), confirming the lower conformational stability of ycc compared to its mammalian homologues.^{36,38,42,43,45–47,60,102–106} The observation of a single cooperative transition from the native to the unfolded form is due to the low ionic strength at which the measurements were made. Indeed, it is known that the stability of molten globule conformer HS2 for horse heart cytochrome *c* increases at high ionic strengths. Under these conditions, two conformational equilibria among the three protein conformers are observed.^{36,38,42,43,46,47}

M80A Variant. The MCD, absorption, and RR spectra of oxidized M80A ycc (M80A hereafter) from pH 7 to 2 are shown in panels a and b of Figures 3 and 4, and in Figure 5, respectively. The UV–vis and MCD spectral parameters are listed in Table 1. At pH 7, the MCD spectrum displays the intense derivative-shaped Soret-related signal typical of a 6c LS ferric heme,^{68,71,76–81,83–89} which is slightly blue-shifted compared to that of wt ycc. The signals in the visible region are generally red-shifted compared to those of wt ycc, and new peaks are observed between 450 and 500 nm. These features are consistent with the replacement of the axial methionine ligand with an OH[–] ion (LS1 conformer), in agreement with literature data.^{54,56,93,96,107} In the high-frequency region of the RR spectra, peaks at 1374 (ν_4), 1502 (ν_3), 1586 (ν_2), and 1636 (ν_{10}) cm^{–1} are characteristic of a 6c LS heme center.⁴ Whereas this part of the spectrum is not significantly different from that of the His/Met wt ycc protein at pH 7, the low-frequency region between 300 and 450 cm^{–1} confirms the identification of a hydroxide as the sixth ligand in the M80A variant,^{93–96,107} because the vibrational band pattern is closely related to that of the His/OH[–]-ligated state of wt ycc formed at pH >10.5

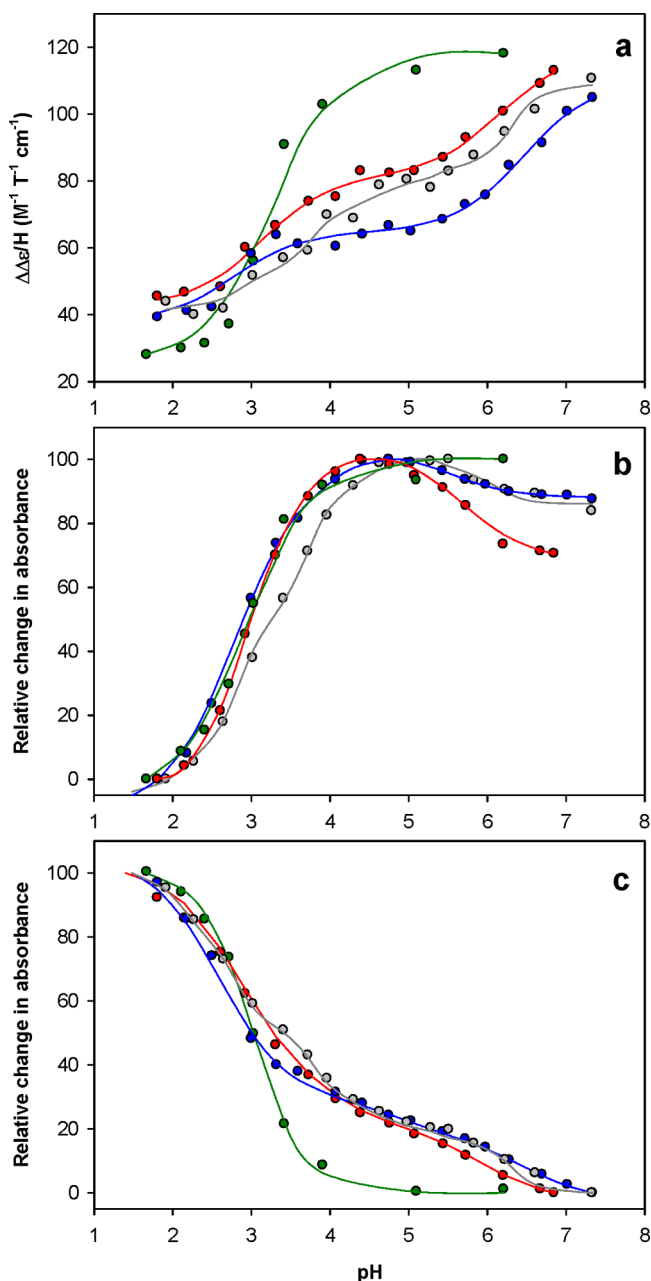


Figure 2. pH-induced changes in (a) the peak-to-trough difference for the MCD signal associated with the Soret band, (b) the relative intensity of the absorbance at 405 nm (408 nm for wt protein), which corresponds to the maximum of the Soret band at neutral pH, and (c) the relative intensity of the absorbance at 394 nm, which corresponds to the maximum of the Soret band at acidic pH for the oxidized form of wild-type (green), M80A (red), M80A/Y67H (blue), and M80/Y67A (gray) *S. cerevisiae* cytochrome *c*. Solid lines are least-squares fits to a one-equilibrium (wt) or a three-equilibria (M80A, M80A/Y67H, and M80A/Y67A) equation.

(Figure 5).¹⁰⁸ Specific spectral markers for the replacement of the Met ligand with a hydroxide are the significant frequency downshift of mode ν_8 by $\sim 5\text{ cm}^{-1}$ to 344 cm^{-1} and the loss of intensity of the prominent band at 398 cm^{-1} .¹⁰⁸

These findings indicate that in M80A a water molecule has taken over the role of Met80 as an axial ligand of the heme and, furthermore, participates in the H-bond network in the heme pocket. At pH 7, the water molecule acts as a proton donor and thus becomes a sufficiently strong ligand (OH^-) to induce a LS

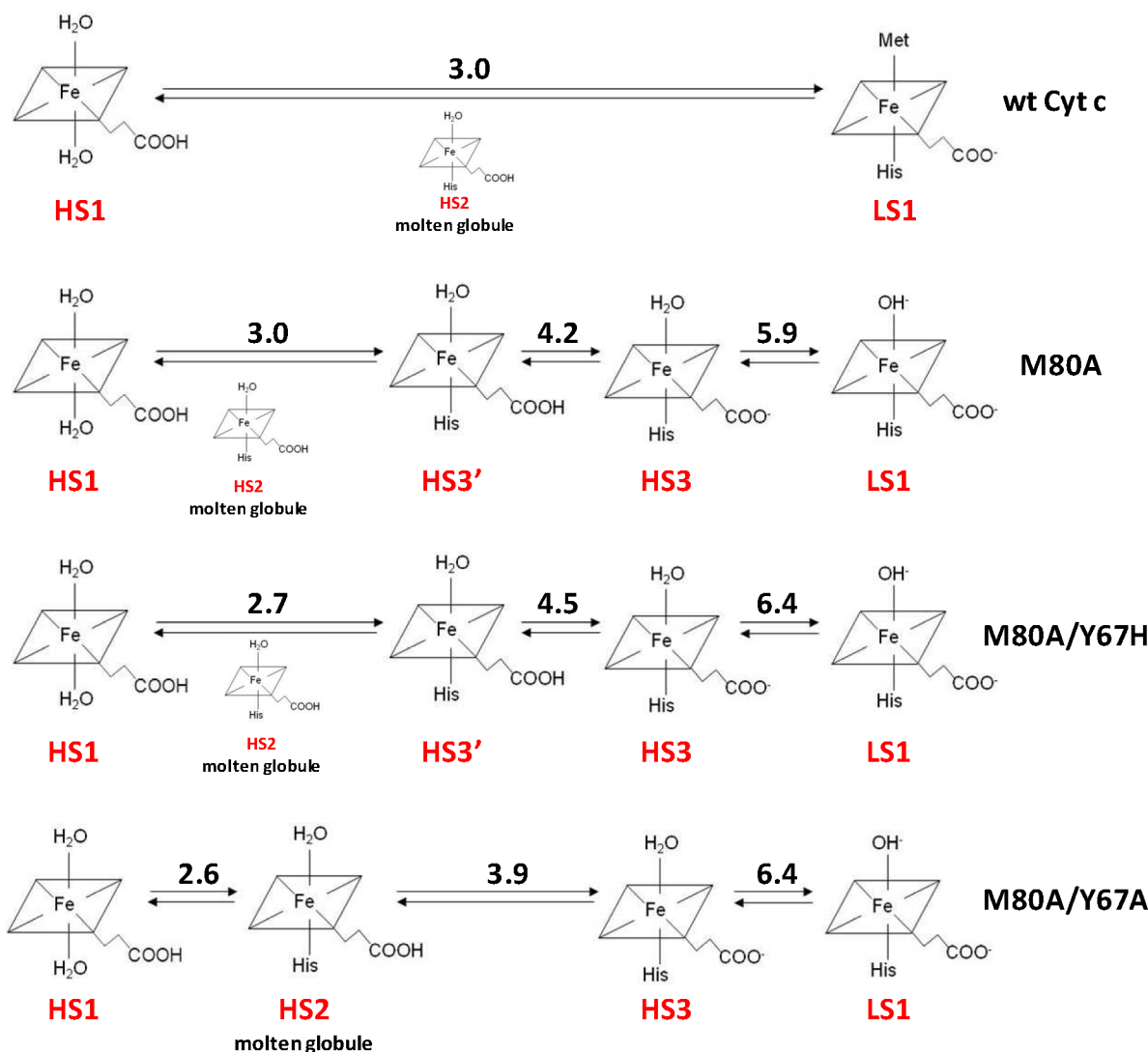
state of the heme iron. Conversely, the hydroxide ligand serves as a proton acceptor below pH 7, contributing to the more complex pH-dependent conformational equilibria of M80A compared to those of wt ycc. When the pH is lowered, at least three additional different conformers can be distinguished.

Lowering the pH to 5 results in a decrease of the peak-to-trough distance and a blue shift of both S-shaped MCD signals (Figures 3a and 4a and Table 1). In addition, an intense trough appears at 630 nm (Figure 4a and Table 1). The Soret absorption band increases in intensity and shifts to shorter wavelengths with an isosbestic point at 408 nm (Figure 3b and Table 1). The α and β bands are replaced by new absorptions, and a new charge-transfer band appears at 621 nm (Figure 4b and Table 1). These variations, due to protonation of the axial OH^- ligand,^{54,56,93,96,107} yield spectral features that are indicative of an equilibrium between low-spin and high-spin 6c ferrihemes,^{68,78,79,83–87,99} corresponding to the transition from LS1 to a high-spin 6c conformer (HS3). This interpretation is confirmed by the RR spectrum at pH 6.2 that demonstrates the rise of two peaks at 1476 and 1568 cm^{-1} , which can be attributed to the ν_3 and ν_2 modes of a His/ H_2O -coordinated HS ferric heme (Figure 5).⁴ The equilibrium is further shifted toward the HS configuration when the pH is lowered. Between pH 5 and 4, the Soret band and the S-shaped MCD signals are slightly blue-shifted (Figures 3a,b and 4a and Table 1), while their intensities and peak-to-trough distances remain nearly unchanged. At pH 3.3, the spectroscopic properties are very similar to those of the HS heme-containing molten globule conformer of native ycc (conformer HS2).

Consistent with the UV-vis and MCD data, the RR spectra show a relative increase in the intensity of the 6c HS marker bands (ν_3 at ca. 1478 cm^{-1} ; ν_2 at 1568 cm^{-1}) at the expense of their 6c LS counterparts at 1502 and 1586 cm^{-1} when the pH is lowered from 6.2 to 3.8 (Figure 5). Note that the intensity ratios of the conjugate bands (i.e., $1478/1502$ and $1568/1586\text{ cm}^{-1}$) are not identical to the 6c HS/6c LS concentration ratio because at 413 nm excitation, which was used in our experiments, the resonance enhancement is stronger for modes of the 6c LS than for those of the 6c HS configuration.⁹⁰

When the pH is further lowered, the spectroscopic properties of M80A dramatically change. At pH 2, the Soret band moves to 394 nm and increases in intensity with an isosbestic at 399 nm , and several changes occur in the visible region (Figures 3b and 4b and Table 1). Moreover, the derivative-shaped MCD Soret signal shifts at shorter wavelengths and becomes less symmetric, and its peak-to-trough distance decreases (Figure 3a and Table 1). These data suggest that at pH 2 the M80A mutant exists as a mixture of two different species, formed by approximately 25% of the HS2 conformer and 75% of a new HS1 form stabilized under strongly acidic conditions. The spectroscopic properties of the latter (obtained by subtracting the contribution of the species stable at higher pH from the experimental spectrum) are very similar to those of the unfolded conformer HS1 of wt ycc under the same conditions, which includes a 6c HS H_2O/H_2O ligand set. Accordingly, the RR spectrum at this pH (Figure 5) shows broad and poorly structured features in the ν_3 and ν_2 mode region with maxima at 1486 and 1573 cm^{-1} , respectively, suggesting the involvement of two different 6c HS configurations. In addition, there may be a small contribution of a 5c HS configuration. The pronounced broadening of modes ν_3 and ν_2 is consistent with a considerable conformational flexibility of the protein matrix surrounding the heme that facilitates ligand exchange.

Scheme 1. pH-Dependent Axial Ligation and Spin State of the Ferric Heme Center for *S. cerevisiae* Iso-1-cytochrome *c* and Its M80A, M80A/Y67H, and M80A/Y67A Variants^a



^aThe average pK_a values, determined from MCD and electronic absorption spectra, are indicated and correspond to each acid–base equilibrium (see the text). Errors in pK_a values are ±0.2.

The pH-induced changes in the peak-to-trough distance of the MCD Soret signal (Figure 2a) and in the relative absorbance of the Soret absorption band at 405 nm (Figure 2b) and 394 nm (Figure 2c) (vide infra) were fit (Scheme 1) by a three-proton equilibrium equation. In order of decreasing pH values, the first equilibrium corresponds to the HS3 ⇌ LS1 transition, which occurs with a pK_a of 5.9 ± 0.2, in close agreement with previously reported values.^{54,93,96,107} The second equilibrium (pK_a = 4.2 ± 0.2) is responsible for the small spectroscopic changes observed between pH 5 and 4. The third is related to the overall HS1 ⇌ HS3 transition, which appears as a single cooperative transition, as for the native protein, with a pK_a of 3.0 ± 0.2. The good agreement of the apparent pK_a values for the HS1 ⇌ HS3 transition of M80A and for the HS1 ⇌ LS1 transition for wt ycc demonstrates that the removal of the axial methionine ligand does not significantly alter the mechanism of acidic unfolding of cytochrome *c* and the intervals of stability of the acidic HS2 and HS1 conformers. Therefore, rupture of the Met80–Fe(III) bond does not trigger the acid unfolding of cytochrome *c*, although breaking of the

same bond is involved in the formation of the molten globule conformer HS2.^{4,36–39,41–44,47,50,51,97} This finding supports the proposal that the acid unfolding of the Ω loop containing the axial Met (i.e., from residue 71 to 85) is triggered by the unfolding of the Ω loop formed by residues 40–57, which in turn is most probably induced by the pH-induced breaking of the H-bond connecting the imidazole ring of His26 with the carboxylate side chain of Glu44.^{27,48,49} Because the structural effect of the M80A mutation is limited to residues in the heme distal cavity,¹⁰⁹ it is conceivable that the interactions described above are not seriously affected by the replacement of the native Met with an Ala.

The acid–base equilibrium influencing the spectroscopic properties of the M80A mutant in the pH range of 3.5–5 is not observed for the wt protein and does not influence the spin state or axial ligation of the heme iron. It is well-known that in mitochondrial cytochromes *c*, the evolutionarily conserved His26 and the heme propionate-7 are characterized by low pK_a values.^{10,110} Spectroscopic studies indicate that in oxidized mitochondrial cytc, the pK_a of His26 is <3.6 as a consequence

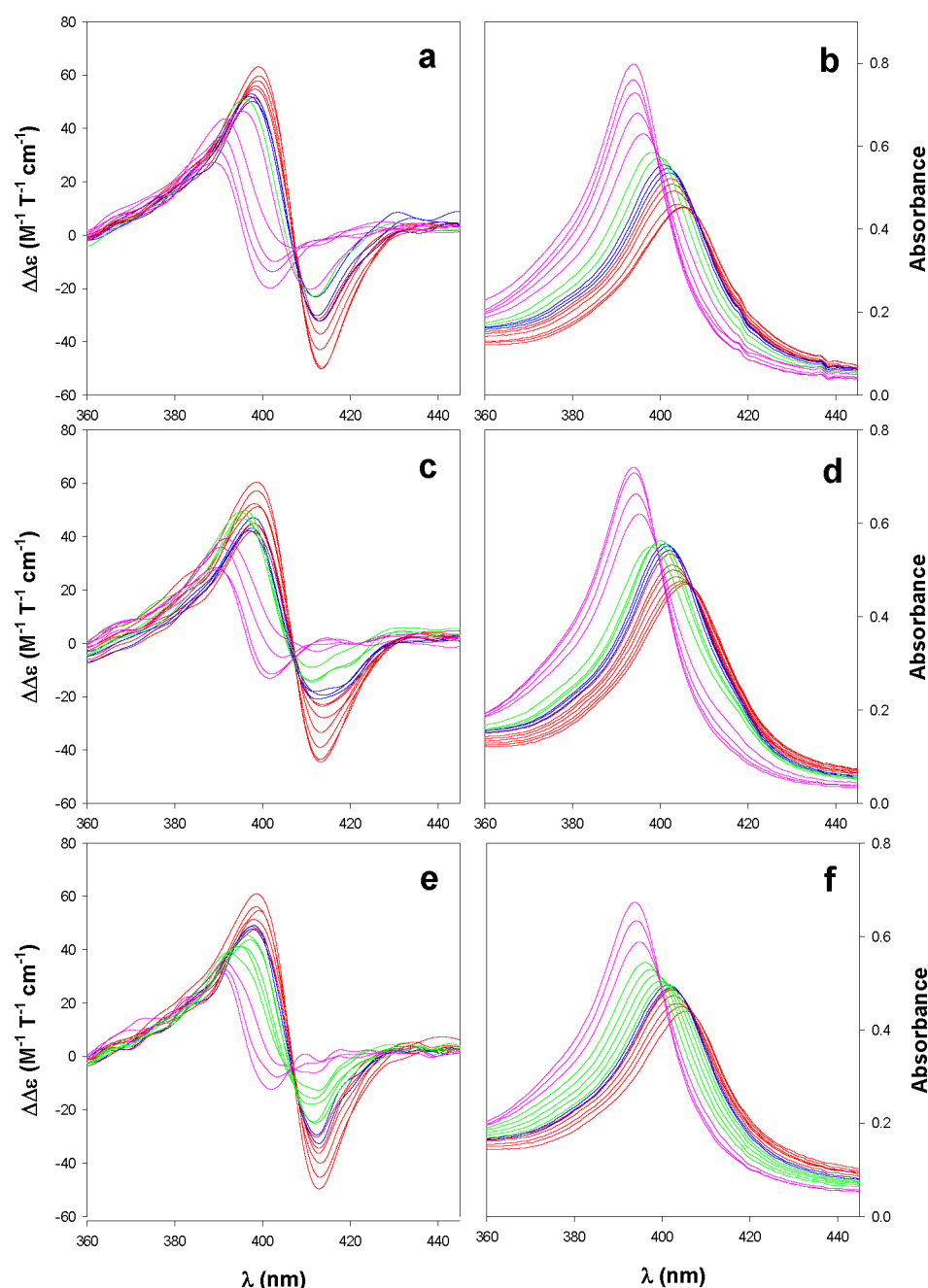


Figure 3. MCD and electronic absorption spectra in the Soret region of the oxidized form of the M80A (a and b), M80A/Y67H (c and d), and M80A/Y67A (e and f) mutants of *S. cerevisiae* cytochrome *c* in 0.5 mM phosphate buffer at different pH values: (a and b) red for $5.0 < \text{pH} < 7.0$, blue for $4.0 < \text{pH} < 5.0$, green for $3.00 < \text{pH} < 3.90$, and pink for $\text{pH} < 3.0$, (c and d) red for $5.0 < \text{pH} < 7.3$, blue for $4.0 < \text{pH} < 5.0$, green for $3.0 < \text{pH} < 3.9$, and pink for $\text{pH} < 3.0$, and (e and f) red for $5.2 < \text{pH} < 7.0$, blue for $4.5 < \text{pH} < 5.2$, green for $3.0 < \text{pH} < 4.5$, and pink for $\text{pH} < 3.0$. Protein concentrations were 20, 20, and 17 μM , respectively.

of its nonpolar environment.^{10,110} Because this environment is conserved in the M80A variant,¹⁰⁹ the pK_a value of His26 should be unaffected by this mutation. On the other hand, the pK_a of the heme propionate-7 in oxidized yeast (and mammalian) cytc is <4.5 , in agreement with the pK_a values of 4.2 ± 0.2 obtained in this study.^{10,110} We therefore propose to assign the intermediate pH-induced transition to the $\text{HS3}' \rightleftharpoons \text{HS3}$ acid–base equilibrium of heme propionate-7 (Scheme 1). The acid–base equilibria involving the heme propionates were not detected by optical spectroscopy in cytochromes *c*, but only in *N*-acetyl microperoxidase-8 and -11.^{66,67,98} The different spectroscopic properties of HS3 and HS2, which share

the same His/ H_2O axial heme ligation, are most probably the result of the different environments surrounding the heme, which can influence the electron donating properties of weak heme axial ligands through H-bonding and electrostatic interactions.⁸⁵ In molten globule conformer HS2, where the heme is surrounded by a folded protein subdomain containing the C- and N-terminal and 60s helices,⁵¹ the electron donating properties of the axial water are weakened compared to those of the HS3 species, suggesting altered H-bonding and electrostatic interactions with the residues in the heme cavity compared to the native form.

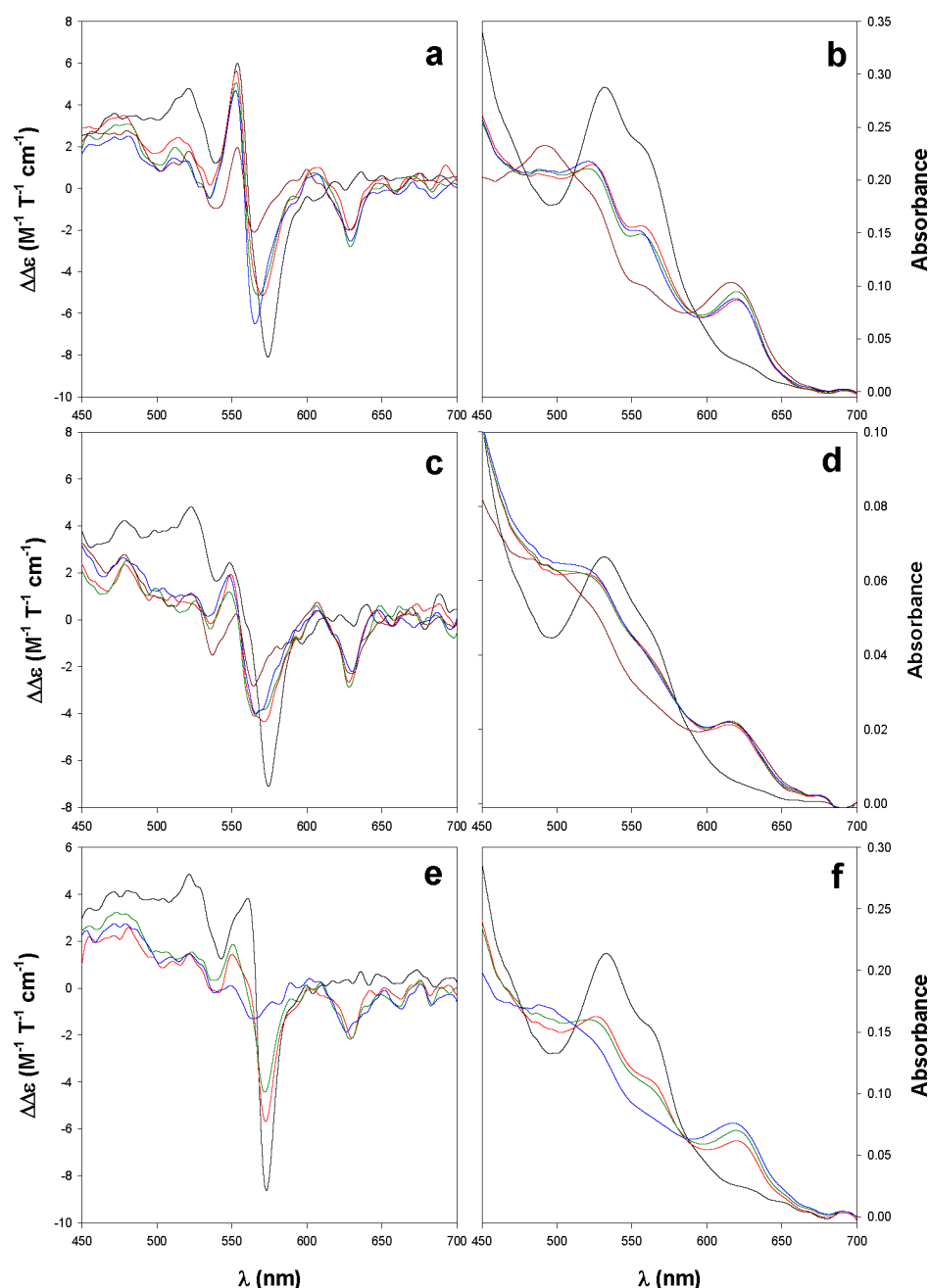


Figure 4. MCD and electronic absorption spectra in the visible region of the oxidized form of the M80A (a and b), M80A/Y67H (c and d), and M80A/Y67A (e and f) mutants of *S. cerevisiae* cytochrome *c* in 0.5 mM phosphate buffer at different pH values: (a and b) black for pH 7.0, red for pH 4.7, green for pH 3.90, blue for pH 3.0, and dark red for pH 2.0, (c and d) black for pH 7.0, red for pH 5.1, green for pH 3.80, blue for pH 2.60, and dark red for pH 2.0, and (e and f) black for pH 7.0, red for pH 5.0, green for pH 3.90, blue for pH 3.0, and dark red for pH 2.0. Protein concentrations were 0.15 mM, 37 μ M, and 0.11 mM, respectively.

M80A/Y67H and M80A/Y67A Variants. The electronic absorption and RR spectra for these double variants are very similar to those for M80A over the whole pH range investigated (Figures 3c–f, 4c–f, and 6 and Table 1), indicating the same pH-dependent coordination changes of the heme center (Scheme 1). It is worth noting that the spectroscopic features of the neutral-pH conformers of both double mutants in the visible region are similar but not identical to those of the corresponding form of M80A, implying that the mutation of Tyr67 affects to some extent the electronic properties of the heme. This is not unexpected as replacement of the side chain of Tyr67 with the imidazole ring of a histidine and the methyl

group of an alanine most likely results in a significant rearrangement of the H-bonding network in the distal heme cavity,⁵ which includes the OH[−]/H₂O heme axial ligand, resulting in an increase in the pK_a values for the LS1 \rightleftharpoons HS3 transition (Scheme 1).

The pH dependencies of the peak-to-trough distance of the MCD Soret signal and the relative absorbance of the Soret band for the LS1 (408 nm) and HS1 conformers (394 nm) for both double variants are reported in Figure 2. The behavior of the M80A/Y67H variant is closely similar to that of the M80A mutant, demonstrating that the electronic properties of the heme are influenced by the same transitions with similar pK_a

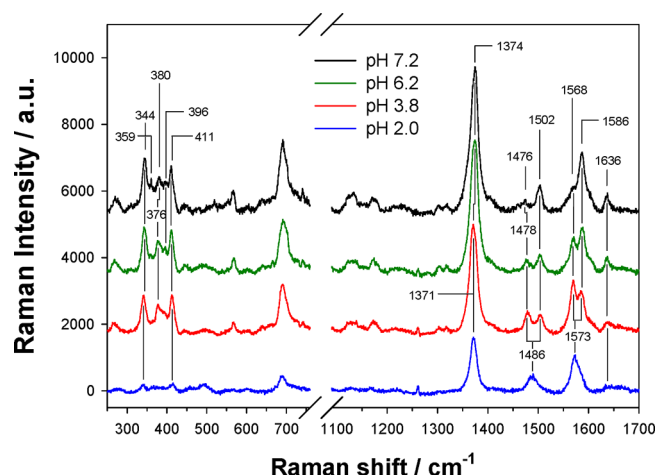


Figure 5. RR spectra of the oxidized form of M80A *S. cerevisiae* cytochrome *c* in a 30 mM phosphate buffer solution at different pH values recorded with a 413 nm excitation line. The spectra were corrected by subtracting a linear baseline. The protein concentration was 160 μ M.

values (Scheme 1). On the other hand, the pH dependencies of M80A/Y67A show significant differences below pH 4.5. In particular, the pH-induced changes in the Soret part of the electronic absorption and MCD spectra observed between pH 4.5 and 3.5 (Table 1, and green spectra in Figure 3e,f) show that HS2 (molten globule) appears at higher pH values than in the other variants, leading to two detectable acid–base equilibria between pH 4.5 and 2 instead of a single cooperative

transition (Figure 2a–c and Scheme 1), as observed for the wt protein at high ionic concentrations or in the presence of chaotropic anions.^{4,36,38–40,42,43,45–47,50,97} In addition, as a result of the increased pK_a for the HS2 \rightleftharpoons HS3 transition, the effects of protonation of heme propionate-7 are not observed.

The slightly lower pK_a value for the overall HS1 \rightleftharpoons HS3' transition in M80A/Y67H compared to those of wt (HS1 \rightleftharpoons LS1) and M80A indicates that replacement of the native tyrosine with a histidine disfavors only slightly the acid unfolding of cyt*c*. This is in agreement with literature data showing that disruption of the H-bonding network connecting the heme propionate-7 with the side chain of Tyr67 enhances the free energy of unfolding and decreases the flexibility of both redox forms of yeast cyt*c*.^{5,57,59,61,62} On the other hand, the increased pK_a for the HS2 \rightleftharpoons HS3 transition in M80A/Y67A shows that the molten globule conformer HS2 is stabilized upon replacement of Tyr67 with Ala. These findings underline the key role played by Tyr67 in stabilizing the 3D structure of cyt*c* by connecting through an H-bonding network the Ω loop running from residue 71 to 85 (containing the axial methionine) with that formed by residues 40–57,^{5,57,59,61,62} which triggers both acid and alkaline unfolding of cyt*c*.^{27,48,64,65} Indeed, the Y67A mutation, perturbing the H-bonding network in the heme pocket, facilitates the formation of molten globule conformer HS2 that precedes the acidic unfolding of cyt*c*.

CONCLUSIONS

The M80A, M80A/Y67H, and M80A/Y67A variants of yeast iso-1-cytochrome *c* undergo more complex low-pH conforma-

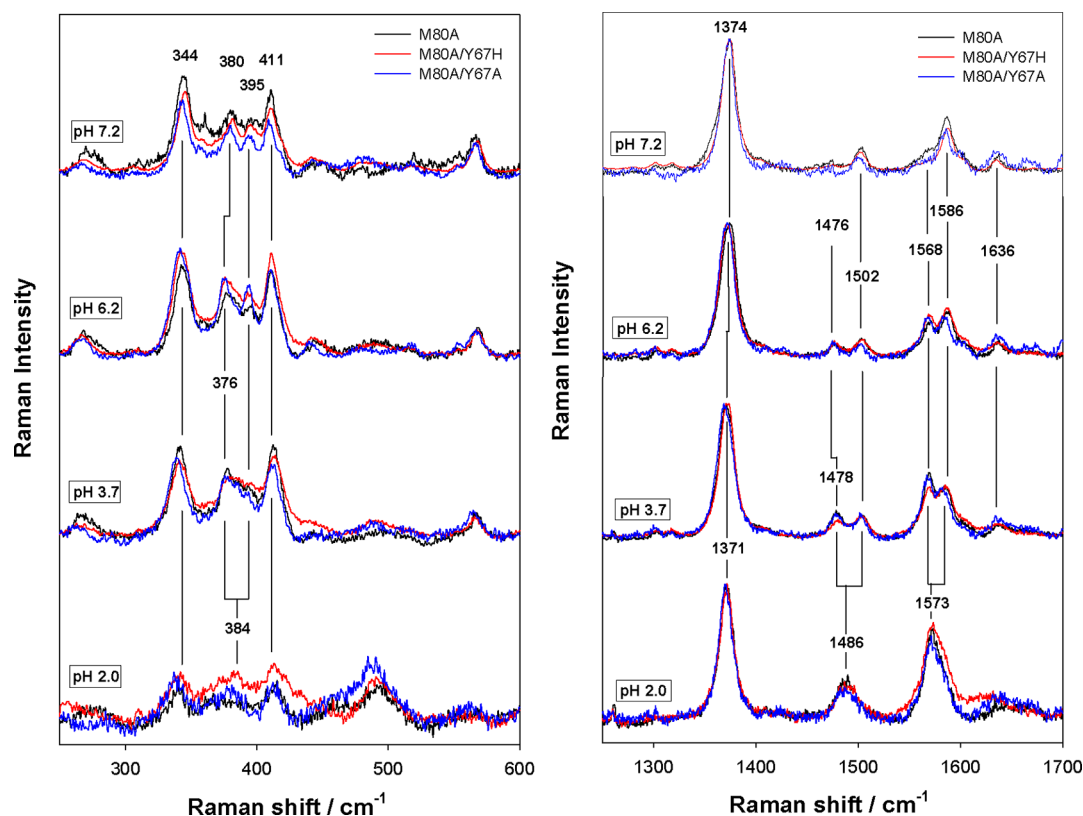


Figure 6. RR spectra of the oxidized forms of the M80A, M80A/Y67H, and M80A/Y67A mutants of *S. cerevisiae* cytochrome *c* between pH 7.2 and 2.0 in the low-frequency (left) and high-frequency (right) regions. Measurements were performed in 30 mM phosphate buffer. The spectra were corrected by subtracting a linear baseline. The protein concentration was 160 μ M.

tional transitions at low ionic strengths than the wt protein. For all mutants, at least four different conformers are observed from pH 7 to 2. In particular, the 6c LS His/OH[−] form observed at neutral pH transforms into a 6c HS His/H₂O-ligated species when the pH is lowered, because of protonation of the axial hydroxide ligand. Two HS conformers whose spectroscopic (and coordination) properties are closely related to the molten globule and to the unfolded state of the native protein are formed below pH 4.5 and 2.5, respectively. The data for the M80A variant show that removal of the axial Met ligand does not significantly alter the mechanism of acidic unfolding of cytc and the pH ranges of stability of the low-pH HS conformers, thereby supporting the view that the acid unfolding of cytc is not triggered by molecular events in the Ω loop containing the axial Met80 ligand. Replacement of Tyr67 with Ala in the M80A/Y67A mutant induces a remarkable change in the low-pH behavior of cytc resulting in the formation of the molten globule HS His/H₂O-ligated conformer at pH values higher than those for the other species. Conversely, no such effect is observed upon substitution of Tyr67 with a His in the M80A/Y67H variant. Thus, Tyr67 stabilizes the 3D structure of cytc by connecting the Ω loops 71–85 and 40–57 through H-bonding. The latter loop triggers both acid and alkaline unfolding of cytc. Therefore, breaking this H-bonding network is the initial key event in the low-pH unfolding of cytc, leading to the formation of the molten globule conformer.

■ ASSOCIATED CONTENT

■ Supporting Information

MCD and electronic absorption spectra for oxidized recombinant wt *S. cerevisiae* cytc in 0.5 mM phosphate buffer at different pH values. This material is available free of charge via the Internet at <http://pubs.acs.org>.

■ AUTHOR INFORMATION

Corresponding Author

*Phone: +39-0592055117. Fax: +39-059373543. E-mail: gianantonio.battistuzzi@unimore.it.

Funding

This work was supported by the Fondazione Cassa di Risparmio di Modena (1297.08.8C) and by the University of Modena and Reggio Emilia (Fondo di Ateneo per la Ricerca, 2009). Financial support by the Leibniz Institute for Molecular Pharmacology in the framework of the Leibniz Graduate School (J.S.) is gratefully acknowledged.

Notes

The authors declare no competing financial interest.

■ REFERENCES

- (1) Jardetzky, O. (1996) Protein dynamics and conformational transitions in allosteric proteins. *Prog. Biophys. Mol. Biol.* 65, 171–219.
- (2) Lanyi, J. K. (1997) Mechanism of ion transport across membranes. Bacteriorhodopsin as a prototype for proton pumps. *J. Biol. Chem.* 272, 31209–31212.
- (3) Parak, F. G. (2003) Proteins in action: The physics of structural fluctuations and conformational changes. *Curr. Opin. Struct. Biol.* 13, 552–557.
- (4) Oellerich, S., Wackerbarth, H., and Hildebrandt, P. (2002) Spectroscopic Characterization of Nonnative Conformational States of Cytochrome *c*. *J. Phys. Chem. B* 106, 6566–6580.
- (5) Ying, T., Wang, Z.-H., Lin, Y.-W., Xie, J., Tan, X., and Huang, Z.-X. (2009) Tyrosine-67 in cytochrome *c* is a possible apoptotic trigger

controlled by hydrogen bonds via a conformational transition. *Chem. Commun.*, 4512–4514.

(6) Valle-Belisle, A., Ricci, F., and Plaxco, K. W. (2009) Thermodynamic basis for the optimization of binding-induced biomolecular switches and structure-switching biosensors. *Proc. Natl. Acad. Sci. U.S.A.* 106, 13802–13807.

(7) Willner, I., and Willner, B. (2001) Photochemical Biomolecular Switches: The Route to Optoelectronics. In *Molecular Switches* (Feringa, B. L., Ed.) Wiley-VCH Verlag GmbH, Weinheim, Germany.

(8) Plaxco, K. W., and Soh, H. T. (2011) Switch-based biosensors: A new approach towards real-time, in vivo molecular detection. *Trends Biotechnol.* 29, 1–5.

(9) Valle-Belisle, A., and Plaxco, K. W. (2010) Structure-switching biosensors: Inspired by Nature. *Curr. Opin. Struct. Biol.* 20, 518–526.

(10) Moore, G. R., and Pettigrew, G. W. (1990) *Cytochromes c. Evolutionary, structural, and physicochemical aspects*, Springer-Verlag, Berlin.

(11) Scott, R. A., and Mauk, A. G., Eds. (1996) *Cytochrome c: A multidisciplinary approach*, University Science Books, Sausalito, CA.

(12) Kagan, V. E., Tyurin, V. A., Jiang, J., Tyurina, Y. Y., Ritov, V. B., Amoscato, A. A., Osipov, A. N., Belikova, N. A., Kapralov, A. A., Kini, V., Vlasova, I. I., Zhao, Q., Zou, M., Di, P., Svistunenko, D. A., Kurnikov, I. V., and Borisenko, G. G. (2005) Cytochrome *c* acts as a cardiolipin oxygenase required for release of proapoptotic factors. *Nat. Chem. Biol.* 1, 223–232.

(13) Sinibaldi, F., Fiorucci, L., Patriarca, A., Lauceri, R., Ferri, T., Coletta, M., and Santucci, R. (2008) Insights into cytochrome *c*–cardiolipin interaction. Role played by ionic strength. *Biochemistry* 47, 6928–6935.

(14) Lutter, M., Fang, M., Luo, X., Nishijima, M., Xie, X.-S., and Wang, X. (2000) Cardiolipin provides specificity for targeting of tBid to mitochondria. *Nat. Cell Biol.* 2, 754–756.

(15) Kluck, R. M., Bossy-Wetzel, E., Green, D. R., and Newmayer, D. D. (1997) The release of cytochrome *c* from mitochondria: A primary site for Bcl-2 regulation of apoptosis. *Science* 275, 1132–1136.

(16) Jang, X., and Wang, X. (2004) Cytochrome *c* mediated apoptosis. *Annu. Rev. Biochem.* 73, 87–106.

(17) Degli Esposti, M. (2004) Mitochondria in apoptosis: Past, present and future. *Biochem. Soc. Trans.* 32, 493–495.

(18) Bradley, J. M., Silkestone, G., Wilson, M. T., Cheesman, M. R., and Butt, J. N. (2011) Probing a complex of cytochrome *c* and cardiolipin by magnetic circular dichroism spectroscopy: Implications for the initial events in apoptosis. *J. Am. Chem. Soc.* 133, 19676–19679.

(19) Rajagopal, B. S., Silkestone, G. C., Nicholls, P., Wilson, M. T., and Worrall, J. A. R. (2012) An investigation into a cardiolipin acyl chain insertion site in cytochrome *c*. *Biochim. Biophys. Acta* 1817, 780–791.

(20) Hanske, J., Toffey, J., Morenz, A. M., Bonilla, A. J., Schiavoni, K. H., and Pletneva, E. V. (2012) Conformational properties of cardiolipin-bound cytochrome *c*. *Proc. Natl. Acad. Sci. U.S.A.* 109, 125–130.

(21) Yeh, S.-R., and Rousseau, D. L. (1999) Ligand exchange during unfolding of cytochrome *c*. *J. Biol. Chem.* 274, 17853–17859.

(22) Yeh, S. R., Han, S., and Rousseau, D. L. (1998) Cytochrome *c* folding and unfolding: A biphasic mechanism. *Acc. Chem. Res.* 31, 727–736.

(23) Yeh, S. R., and Rousseau, D. L. (1998) Folding intermediates in cytochrome *c*. *Nat. Struct. Biol.* 5, 222–228.

(24) Takahashi, S., Yeh, S. R., Das, T. K., Chan, C.-K., Gottfried, D. S., and Rousseau, D. (1997) Folding of cytochrome *c* initiated by submillisecond mixing. *Nat. Struct. Biol.* 4, 44–50.

(25) Yeh, S. R., Takahashi, S., Fan, B. C., and Rousseau, D. L. (1997) Ligand exchange during cytochrome *c* folding. *Nat. Struct. Biol.* 4, 51–56.

(26) Englander, S. W., Sosnick, T. R., Mayne, L. C., Shtilerman, M., Qi, P. X., and Bai, Y. (1998) Fast and slow folding in cytochrome *c*. *Acc. Chem. Res.* 31, 737–744.

(27) Krishna, M. M. G., Lin, Y., Rumbley, J. N., and Englander, S. W. (2003) Cooperative Ω loops in cytochrome *c*: Role in folding and function. *J. Mol. Biol.* 331, 29–36.

- (28) Thomas, Y. G., Goldbeck, R. A., and Kliger, D. S. (2000) Characterization of equilibrium intermediates in denaturant-induced unfolding of ferrous and ferric cytochromes *c* using magnetic circular dichroism, circular dichroism, and optical absorption spectroscopies. *Biopolymers* 57, 29–36.
- (29) Nakamura, S., Seki, Y., Katoh, E., and Kidokoro, S.-I. (2011) Thermodynamic and structural properties of the acid molten globule state of horse cytochrome *c*. *Biochemistry* 50, 3116–3126.
- (30) Xu, Q., and Keiderling, T. A. (2004) Optical spectroscopic differentiation of various equilibrium denatured states of horse cytochrome *c*. *Biopolymers* 73, 716–726.
- (31) Duncan, M. G., Williams, M. D., and Bowler, B. E. (2009) Compressing the free energy range of substructure stabilities in iso-1-cytochrome *c*. *Protein Sci.* 18, 1155–1164.
- (32) Pletneva, E. V., Gray, H. B., and Winkler, J. R. (2005) Many faces of the unfolded state: Conformational heterogeneity in denatured yeast cytochrome *c*. *J. Mol. Biol.* 345, 855–867.
- (33) Pletneva, E. V., Gray, H. B., and Winkler, J. R. (2005) Nature of the cytochrome *c* molten globule. *J. Am. Chem. Soc.* 127, 15370–15371.
- (34) Nall, B. T. (1996) Cytochrome *c* folding and stability. In *Cytochrome c: A multidisciplinary approach* (Scott, R. A., and Mauk, A. G., Eds.) pp 167–200, University Science Books, Sausalito, CA.
- (35) Wilson, M. T., and Greenwood, C. (1996) The Alkaline Transition in Ferricytochrome *c*. In *Cytochrome c: A multidisciplinary approach* (Scott, R. A., and Mauk, A. G., Eds.) pp 611–634, University Science Books, Sausalito, CA.
- (36) Goto, Y., Takahashi, N., and Finks, A. L. (1990) Mechanism of acid-induced folding of proteins. *Biochemistry* 29, 3480–3488.
- (37) Goto, Y., Calciano, L. J., and Fink, A. L. (1990) Acid-induced folding of proteins. *Proc. Natl. Acad. Sci. U.S.A.* 87, 573–577.
- (38) Goto, Y., Hagihara, Y., Hamada, D., Hoshino, M., and Nishii, I. (1993) Acid-induced unfolding and refolding transitions of cytochrome *c*: A three-state mechanism in H₂O and D₂O. *Biochemistry* 32, 11878–11885.
- (39) Szewczuk, Z., Konishi, Y., and Goto, Y. (2001) A two-process model describes the hydrogen exchange behavior of cytochrome *c* in the molten globule state with various extents of acetylation. *Biochemistry* 40, 9623–9630.
- (40) Greenwood, C., and Wilson, M. T. (1971) Studies on Ferricytochrome *c*. I. Effect of pH, Ionic Strength and Protein Denaturants on the Spectra of Ferricytochrome *c*. *Eur. J. Biochem.* 22, 5–10.
- (41) Babul, J., and Stellwagen, E. (1972) Participation of the protein ligands in the folding of cytochrome *c*. *Biochemistry* 11, 1195–1200.
- (42) Stellwagen, E., and Babul, J. (1975) Stabilization of the globular structure of ferricytochrome *c* by chloride in acidic solvents. *Biochemistry* 14, 5135–5140.
- (43) Aviram, I. (1973) The interaction of chaotropic anions with acid ferricytochrome *c*. *J. Biol. Chem.* 248, 1891–1896.
- (44) Lanir, A., Yu, N.-T., and Felton, R. H. (1979) Conformational transitions and vibronic couplings in acid ferricytochrome *c*: A resonance Raman study. *Biochemistry* 18, 1656–1660.
- (45) Robinson, J. B., Jr., Strottmann, J. M., and Stellwagen, E. (1983) A globular high spin form of ferricytochrome *c*. *J. Biol. Chem.* 258, 6772–6776.
- (46) Dyson, H. J., and Beattie, J. K. (1982) Spin state and unfolding equilibria of ferricytochrome *c* in acidic solutions. *J. Biol. Chem.* 257, 2267–2273.
- (47) Stupak, M., Bagelova, J., Fedunova, D., and Antalík, M. (2006) Conformational transitions of ferricytochrome *c* in strong inorganic acids. *Collect. Czech. Chem. Commun.* 71, 1627–1641.
- (48) Baddam, S., and Bowler, B. E. (2006) Mutation of asparagine 52 to glycine promotes the alkaline form of iso-1-cytochrome *c* and causes loss of cooperativity in acid unfolding. *Biochemistry* 45, 4611–4619.
- (49) Sinibaldi, F., Piro, M. C., Howes, B. D., Smulevich, G., Ascoli, F., and Santucci, R. (2003) Rupture of the hydrogen bond linking two Ω -loops induces the molten globule state at neutral pH in cytochrome *c*. *Biochemistry* 42, 7604–7610.
- (50) Sinibaldi, F., Howes, B. D., Smulevich, G., Ciaccio, C., Coletta, M., and Santucci, R. (2003) Anion concentration modulates the conformation and stability of the molten globule of cytochrome *c*. *J. Biol. Inorg. Chem.* 8, 663–670.
- (51) Jordan, T., Eads, J. C., and Spiro, T. G. (1995) Secondary and tertiary structure of the A-state of cytochrome *c* from resonance Raman spectroscopy. *Protein Sci.* 4, 716–728.
- (52) Pineda, T., Sevilla, J. M., Roman, A. J., and Blazquez, M. (1997) Electrochemical evidence on the molten globule conformation of cytochrome *c*. *Biochim. Biophys. Acta* 1343, 227–234.
- (53) Bortolotti, C. A., Battistuzzi, G., Borsari, M., Facci, P., Ranieri, A., and Sola, M. (2006) The redox chemistry of the covalently immobilized native and low-pH forms of yeast iso-1-cytochrome *c*. *J. Am. Chem. Soc.* 128, 5444–5451.
- (54) Casalini, S., Battistuzzi, G., Borsari, M., Bortolotti, C. A., Ranieri, A., and Sola, M. (2008) Electron transfer and electrocatalytic properties of the immobilized methionine80alanine cytochrome *c* variant. *J. Phys. Chem. B* 112, 1555–1563.
- (55) Casalini, S., Battistuzzi, G., Borsari, M., Ranieri, A., and Sola, M. (2008) Catalytic reduction of dioxygen and nitrite ion at a Met80Ala cytochrome *c*-functionalized electrode. *J. Am. Chem. Soc.* 130, 15099–15104.
- (56) Casalini, S., Battistuzzi, G., Borsari, M., Bortolotti, C. A., Di Rocco, G., Ranieri, A., and Sola, M. (2010) Electron transfer properties and hydrogen peroxide electrocatalysis of cytochrome *c* variants at positions 67 and 80. *J. Phys. Chem. B* 114, 1698–1706.
- (57) Berghuis, A., Guillemette, J. G., Smith, M. I., and Brayer, G. D. (1994) Mutation of tyrosine-67 to phenylalanine in cytochrome *c* significantly alters the local heme environment. *J. Mol. Biol.* 235, 1326–1341.
- (58) Raja Singh, S., Prakash, S., Vasu, V., and Karunakaran, C. (2009) Conformational flexibility decreased due to Y67F and F82H mutations in cytochrome *c*: Molecular dynamics simulation studies. *J. Mol. Graphics Modell.* 28, 270–277.
- (59) Lett, C. M., Berghuis, A. M., Frey, H. E., Lepock, J. R., and Guillemette, J. G. (1996) The role of a conserved water molecule in the redox-dependent thermal stability of iso-1-cytochrome *c*. *J. Biol. Chem.* 271, 29088–29093.
- (60) Lett, C. M., Rosu-Myles, M. D., Frey, H. E., and Guillemette, J. G. (1999) Rational design of a more stable yeast iso-1-cytochrome *c*. *Biochim. Biophys. Acta* 1432, 40–48.
- (61) Schejter, A., Luntz, T. L., Koshy, T. I., and Margoliash, E. (1992) Relationship between local and global stabilities of proteins: Site-directed mutants and chemically-modified derivatives of cytochrome *c*. *Biochemistry* 31, 8336–8343.
- (62) Luntz, T. L., Schejter, A., Garber, E. A. E., and Margoliash, E. (1989) Structural significance of an internal water molecule studied by site-directed mutagenesis of tyrosine-67 in rat cytochrome *c*. *Proc. Natl. Acad. Sci. U.S.A.* 86, 3524–3528.
- (63) Feinberg, B. A., Petro, L., Hock, G., Qin, W., and Margoliash, E. (1999) Using entropies of reaction to predict changes in protein stability: Tyrosine-67-phenylalanine variants of rat cytochrome *c* and yeast iso-1 cytochromes *c*. *J. Pharm. Biomed. Anal.* 19, 115–125.
- (64) Baddam, S., and Bowler, B. E. (2005) Thermodynamics and kinetics of formation of the alkaline state of a Lys79/Ala Lys73/His variant of iso-1-cytochrome *c*. *Biochemistry* 44, 14956–14968.
- (65) Godbole, S., and Bowler, B. E. (1999) Effect of pH on formation of a natively intermediate on the unfolding pathway of a Lys73/His variant of yeast iso-1-cytochrome *c*. *Biochemistry* 38, 487–495.
- (66) Marques, H. M. (2007) Insights into porphyrin chemistry provided by the microperoxidases, the haempeptides derived from cytochrome *c*. *Dalton Trans.*, 4371–4385.
- (67) Munro, O. Q., and Marques, H. M. (1996) Heme-peptide models for hemoproteins. I. Solution chemistry of N-acetylmicroperoxidase-8. *Inorg. Chem.* 35, 3752–3767.
- (68) Pond, A. E., Sono, M., Elenkova, E. A., McRee, D. E., Goodin, D. B., English, A. M., and Dawson, J. H. (1999) Magnetic circular dichroism studies of the active site heme coordination sphere of

exogenous ligand-free ferric cytochrome *c* peroxidase from yeast: Effects of sample history and pH. *J. Inorg. Biochem.* 76, 165–174.

(69) Paulat, F., and Lehnert, N. (2008) Detailed assignment of the magnetic circular dichroism and UV-vis spectra of five-coordinate high-spin ferric [Fe(TPP)(Cl)]. *Inorg. Chem.* 47, 4963–4976.

(70) Kirk, M. L., and Peariso, K. (2003) Recent applications of MCD spectroscopy to metalloenzymes. *Curr. Opin. Chem. Biol.* 7, 220–227.

(71) Walker, F. A. (1999) Magnetic spectroscopic (EPR, ESEEM, Mossbauer, MCD and NMR) studies of low-spin ferriheme centers and their corresponding heme proteins. *Coord. Chem. Rev.* 185–186, 471–534.

(72) McMaster, J., and Oganessian, V. S. (2010) Magnetic circular dichroism spectroscopy as a probe of the structures of the metal sites in metalloproteins. *Curr. Opin. Struct. Biol.* 20, 615–622.

(73) Cheesman, M. R., Greenwood, C., and Thomson, A. J. (1991) Magnetic circular dichroism of hemoproteins. *Adv. Inorg. Chem.* 36, 201–255.

(74) Cheek, J., and Dawson, J. H. (2000) Magnetic circular dichroism spectroscopy of heme proteins and model systems. In *Porphyrin Handbook* (Kadish, K. M., Smith, K. M., and Guillard, R., Eds.) pp 339–369, Academic Press, San Diego.

(75) Johnson, M. K. (2000) CD and MCD Spectroscopy. In *Physical methods in bioinorganic chemistry* (Que, L., Jr., Ed.) pp 233–286, University Science Books, Sausalito, CA.

(76) Vickery, L., Nozawa, T., and Sauer, K. (1976) Magnetic circular dichroism studies of low-spin cytochromes. Temperature dependence and effects of axial coordination on the spectra of cytochrome *c* and cytochrome *b₅*. *J. Am. Chem. Soc.* 98, 351–357.

(77) Vickery, L., Nozawa, T., and Sauer, K. (1976) Magnetic circular dichroism studies of myoglobin complexes. Correlations with heme spin state and axial ligation. *J. Am. Chem. Soc.* 98, 343–350.

(78) Du, J., Sono, M., and Dawson, J. H. (2011) The H93G myoglobin cavity mutant as a versatile scaffold for modeling heme iron coordination structures in protein active sites and their characterization with magnetic circular dichroism spectroscopy. *Coord. Chem. Rev.* 255, 700–716.

(79) Du, J., Perera, R., and Dawson, J. H. (2011) Alkylamine-Ligated H93G Myoglobin Cavity Mutant: A Model System for Endogenous Lysine and Terminal Amine Ligation in Heme Proteins such as Nitrite Reductase and Cytochrome *f*. *Inorg. Chem.* 50, 1242–1249.

(80) Fedurco, M., Augustynski, J., Indiani, C., Smulevich, G., Antalík, M., Bano, M., Sedlak, E., Glascock, M. C., and Dawson, J. H. (2004) The heme iron coordination of unfolded ferric and ferrous cytochrome *c* in neutral and acidic urea solutions. Spectroscopic and electrochemical studies. *Biochim. Biophys. Acta* 1703, 31–41.

(81) Fedurco, M., Augustynski, J., Indiani, C., Smulevich, G., Antalík, M., Bano, M., Sedlak, E., Glascock, M. C., and Dawson, J. H. (2005) Electrochemistry of unfolded cytochrome *c* in neutral and acidic urea solutions. *J. Am. Chem. Soc.* 127, 7638–7646.

(82) Droghetti, E., Sumithran, S., Sono, M., Antalík, M., Fedurco, M., Dawson, J. H., and Smulevich, G. (2009) Effects of urea and acetic acid on the heme axial ligation structure of ferric myoglobin at very acidic pH. *Arch. Biochem. Biophys.* 489, 68–75.

(83) Dawson, J. H., Pond, A. E., and Roach, M. P. (2002) H93G myoglobin cavity mutant as versatile template for modeling heme proteins: Magnetic circular dichroism studies of thiolate- and imidazole-ligated complexes. *Biopolymers* 67, 200–206.

(84) Pond, A. E., Roach, M. P., Thomas, M. R., Boxer, S. G., and Dawson, J. H. (2000) The H93G myoglobin cavity mutant as a versatile template for modeling heme proteins: Ferrous, ferric, and ferryl mixed-ligand complexes with imidazole in the cavity. *Inorg. Chem.* 39, 6061–6066.

(85) Pond, A. E., Sono, M., Elenkova, E. A., Goodin, D. B., English, A. M., and Dawson, J. H. (1999) Influence of protein environment on magnetic circular dichroism spectral properties of ferric and ferrous ligand complexes of yeast cytochrome *c* peroxidase. *Biospectroscopy* 5, S42–S52.

(86) Pond, A. E., Roach, M. P., Sono, M., Huff Rux, A., Franzen, S., Hu, R., Thomas, M. R., Wilks, A., Dou, Y., Ikeda-Saito, M., Ortiz de

Montellano, P. R., Woodruff, W. H., Boxer, S. G., and Dawson, J. H. (1999) Assignment of the heme axial ligand(s) for the ferric myoglobin (H93G) and heme oxygenase (H25A) cavity mutants as oxygen donors using magnetic circular dichroism. *Biochemistry* 38, 7601–7608.

(87) Dawson, J. H., Kadkhodayan, S., Zhuang, C., and Sono, M. (1992) On the use of iron octa-alkylporphyrins as models for protoporphyrin IX-containing heme systems in studies employing magnetic circular dichroism spectroscopy. *J. Inorg. Biochem.* 45, 179–192.

(88) Kintner, E. T., and Dawson, J. H. (1991) Spectroscopic studies of ferric porphyrins with quantum mechanically admixed intermediate-spin states: Models for cytochrome *c*'. *Inorg. Chem.* 30, 4892–4897.

(89) Rux, J. J., and Dawson, J. H. (1991) Magnetic circular dichroism spectroscopy as a probe for axial heme ligand replacement in semisynthetic mutants of cytochrome *c*. *FEBS Lett.* 290, 49–51.

(90) Ly, H. K., Utesch, T., Díaz-Moreno, I., García-Heredia, J. M., De La Rosa, M. A., and Hildebrandt, P. (2012) Perturbation of the redox site structure of cytochrome *c* variants upon tyrosine nitration. *J. Phys. Chem. B* 116, 5694–5702.

(91) Siebert, F., and Hildebrandt, P. (2007) *Vibrational spectroscopy in life science*, Wiley-VCH, Weinheim, Germany.

(92) Margoliash, E., and Frohwirt, N. (1959) Spectrum of horse-heart cytochrome *c*. *Biochem. J.* 71, 570–572.

(93) Bren, K. L., and Gray, H. B. (1993) Structurally engineered cytochromes with novel ligand binding sites: Oxy and carbon monoxide derivatives of semisynthetic horse heart Ala80 cytochrome *c*. *J. Am. Chem. Soc.* 115, 10382–10383.

(94) Sutherland, J. C., and Klein, M. P. (1972) Magnetic Circular Dichroism of Cytochrome *c*. *J. Chem. Phys.* 57, 76–86.

(95) Riesler, J.-L., and Groudinsky, O. (1973) Magnetic circular dichroism studies of cytochrome *c* and cytochrome *b₅*. *Eur. J. Biochem.* 35, 201–205.

(96) Banci, L., Bertini, I., Bren, K., Gray, H. B., and Turano, P. (1995) pH-dependent equilibria of yeast Met80Ala-iso-1 cytochrome *c* probed by NMR spectroscopy: A comparison with the wild-type protein. *Chem. Biol.* 2, 377–383.

(97) Santucci, R., Bongiovanni, C., Mei, G., Ferri, T., Polizio, F., and Desideri, A. (2000) Anion size modulates the structure of the A state of cytochrome *c*. *Biochemistry* 39, 12632–12638.

(98) Marques, H. M., and Perry, C. B. (1999) Hemepeptide models for hemoproteins: The behavior of N-acetylmicroperoxidase-11 in aqueous solution. *J. Inorg. Biochem.* 75, 281–291.

(99) Cheek, J., Low, D. W., Gray, H. B., and Dawson, J. H. (1998) Histidine-tailed microperoxidase-10: A pH-dependent ligand switch. *Biochem. Biophys. Res. Commun.* 253, 195–198.

(100) Wang, J.-S., Tsai, A.-L., Heldt, J., Palmer, G., and Van Wart, H. E. (1992) Temperature- and pH-dependent changes in the coordination sphere of the heme *c* group in the model peroxidase N^α-acetyl microperoxidase-8. *J. Biol. Chem.* 267, 15310–15318.

(101) Polastro, E., Looze, Y., and Léonis, J. (1976) Study of the biological significance of cytochrome methylation I. Thermal, acid and guanidinium hydrochloride denaturations of baker's yeast ferricytochromes *c*. *Biochim. Biophys. Acta* 446, 310–320.

(102) Cohen, D. S., and Pielak, G. J. (1994) Stability of yeast iso-1 ferricytochrome *c* as a function of pH and temperature. *Protein Sci.* 3, 1253–1260.

(103) Endo, S., Nagayama, K., and Wada, A. (1985) Probing stability and dynamics of proteins by protease digestion. I: Comparison of protease susceptibility and thermal stability of cytochromes *c*. *J. Biomol. Struct. Dyn.* 3, 409–421.

(104) Koshy, T. L., Luntz, T. L., Plotkin, B., Schejter, A., and Margoliash, E. (1994) The significance of denaturant titrations of protein stability: A comparison of rat and baker's yeast cytochrome *c* and their site-directed asparagine-52-to-isoleucine mutants. *Biochem. J.* 299, 347–350.

(105) Margoliash, E., and Schejter, A. (1966) Cytochrome *c*. *Adv. Protein Chem.* 21, 113–286.

- (106) Aviram, I., and Schejter, A. (1969) Physicochemical properties of baker's yeast iso-1-cytochrome *c*. *J. Biol. Chem.* 244, 3773–3778.
- (107) Lu, Y., Casimiro, D. R., Bren, K. L., Richards, J. H., and Gray, H. B. (1993) Structurally expressed cytochromes with novel ligand binding properties: Expression of *Saccharomyces cerevisiae* Met-80 → Ala iso-1-cytochrome *c*. *Proc. Natl. Acad. Sci. U.S.A.* 90, 11456–11459.
- (108) Döpner, S., Hildebrandt, P., Rosell, F. I., and Mauk, A. G. (1998) Alkaline Conformational Transitions of Ferricytochrome *c* Studied by Resonance Raman Spectroscopy. *J. Am. Chem. Soc.* 120, 11246–11255.
- (109) Banci, L., Bertini, I., Bren, K. L., Gray, H. B., Sompornpisut, P., and Turano, P. (1995) Three-dimensional solution structure of the cyanide adduct of a Met80Ala variant of *Saccharomyces cerevisiae* iso-1-cytochrome *c*. Identification of ligand-residue interactions in the distal heme cavity. *Biochemistry* 34, 11385–11398.
- (110) Pielak, G. J., Auld, D. S., Betz, S. F., Hilgen-Willis, S. E., and Garcia, L. L. (1996) Nuclear Magnetic Resonance Studies of Class I Cytochromes *c*. In *Cytochrome c: A multidisciplinary approach* (Scott, R. A., and Mauk, A. G., Eds.) pp 203–284, University Science Books, Sausalito, CA.